Chemosphere 321 (2023) 138133

Contents lists available at ScienceDirect

Chemosphere

journal homepage: www.elsevier.com/locate/chemosphere

Effect of pH, surface charge and soil properties on the solid–solution partitioning of perfluoroalkyl substances (PFASs) in a wide range of temperate soils

Hugo Campos-Pereira [a], Dan B. Kleja [a,b], Lutz Ahrens [c], Anja Enell [b], Johannes Kikuchi [b,d], Michael Pettersson [b], Jon Petter Gustafsson [a,*]

[a] Department of Soil and Environment, Swedish University of Agricultural Sciences (SLU), Box 7014, SE-750 07, Uppsala, Sweden
[b] Swedish Geotechnical Institute (SGI), SE-581 93, Linköping, Sweden
[c] Department of Aquatic Sciences and Assessment, Swedish University of Agricultural Sciences (SLU), Box 7050, SE-750 07, Uppsala, Sweden
[d] Department of Thematic Studies, Linköping University, SE-581 83, Linköping, Sweden

HIGHLIGHTS

- pH-dependent partitioning of six PFASs was studied for eleven temperate mineral soils.
- The pH dependence of sorption increased with the length of the perfluorocarbon chain.
- Organic carbon (OC) alone was a poor predictor of PFAS sorption.
- Multiple regression suggested sorption contributions from OC and metal oxides.
- A model predicting PFAS sorption from net organic charge underestimated K_d.

GRAPHICAL ABSTRACT

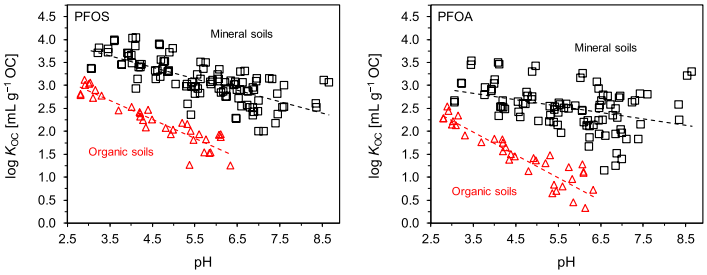

ARTICLE INFO

Handling Editor: Magali Houde

Keywords:
PFOS
PFOA
Sorption
Binding
Organic matter
Geochemical modeling

ABSTRACT

The pH-dependent soil–water partitioning of six perfluoroalkyl substances (PFASs) of environmental concern (PFOA, PFDA, PFUnDA, PFHxS, PFOS and FOSA), was investigated for 11 temperate mineral soils and related to soil properties such as organic carbon content (0.2–3%), concentrations of Fe and Al (hydr)oxides, and texture. PFAS sorption was positively related to the perfluorocarbon chain length of the molecule, and inversely related to solution pH for all substances. The negative slope between log K_d and pH became steeper with increasing perfluorocarbon chain length of the PFAS ($r^2 = 0.75$, $p \leq 0.05$). Organic carbon (OC) alone was a poor predictor of the partitioning for all PFASs, except for FOSA ($r^2 = 0.71$), and the OC-normalized PFAS partitioning, as derived from organic soil materials, underestimated PFAS sorption to the soils. Multiple linear regression suggested sorption contributions ($p \leq 0.05$) from OC for perfluorooctane sulfonate (PFOS) and FOSA, and Fe/Al (hydr) oxides for PFOS, FOSA, and perfluorodecanoate (PFDA). FOSA was the only substance under study for which there was a statistically significant correlation between its binding and soil texture (silt + clay). To predict PFAS sorption, the surface net charge of the soil organic matter fraction of all soils was calculated using the Stockholm Humic Model. When calibrated against charge-dependent PFAS sorption to a peat (Oe) material, the derived model significantly underestimated the measured K_d values for 10 out of 11 soils. To conclude, additional

* Corresponding author.
E-mail address: jon-petter.gustafsson@slu.se (J.P. Gustafsson).

https://doi.org/10.1016/j.chemosphere.2023.138133
Received 29 October 2022; Received in revised form 9 February 2023; Accepted 10 February 2023
Available online 13 February 2023

sorbents, possibly including silicate minerals, contribute to the binding of PFASs in soil. More research is needed to develop geochemical models that can accurately predict PFAS sorption in soils.

1. Introduction

The persistence, large environmental mobility, and toxicity of perfluoroalkyl substances (PFASs) highlight a need for more accurate environmental risk assessments. However, to perform robust long-term risk assessments, it is necessary to have a better understanding of the binding mechanisms in soils and to what extent PFAS mobility changes with geochemical conditions. It is now well established that the perfluorocarbon chain length in PFAS molecules, which reflects the intrinsic hydrophobicity, is closely related to the overall sorption of the substance (Guelfo et al., 2021; Guelfo and Higgins, 2013; Nguyen et al., 2020). Further, the soil solution pH has a substantial impact on PFAS binding due to the pH-dependent charge of common sorbents such as organic matter and Fe and Al (hydr)oxides (e.g., Nguyen et al., 2020; Higgins and Luthy, 2006; Campos-Pereira et al., 2020, 2022). This has been attributed to charge interactions between the particulate phase and PFAS (Nguyen et al., 2020; Higgins and Luthy, 2007). However, the mechanisms governing the magnitude of pH- and charge-dependent PFAS binding are not yet fully understood. Moreover, the pH-dependent sorption of PFASs, such as perfluorooctane sulfonamide (FOSA), which change their protonation state over the environmentally relevant pH range, has been described only to a limited extent in the current literature (Mejia-Avendaño et al., 2020; Nguyen et al., 2020; Zhi and Liu, 2018). This is despite the fact that the change in protonation state may substantially alter the binding, leaching and fate of FOSA in the environment.

In many studies, organic matter (measured as organic carbon, OC) has been found to be an important sorbent for PFASs (e.g., Umeh et al., 2021; Nguyen et al., 2020). However, OC alone has rarely been reported to strongly correlate with soil-pore water distribution coefficients (K_d) for PFAS (Umeh et al., 2021; Li et al., 2018), although OC has been found to be a better predictor for the sorption of longer-chained as compared to that of shorter-chained PFASs (Nguyen et al., 2020). The relative roles of soil components such as organic carbon (Campos-Pereira et al., 2022; Fabregat-Palau et al., 2022; Zhi and Liu, 2018), Fe- and Al (hydr)oxides (Campos-Pereira et al., 2020; Oliver et al., 2019; Tang et al., 2010; Wang and Shih, 2011), and clay minerals (Xiao et al., 2011; Jeon et al., 2011; Luft et al., 2022) remain to be fully understood, especially with regards to how their relative contributions change when the soil pH changes in natural and engineered systems (e.g., upon soil washing). While the sorption of many PFASs onto organic matter and metal (hydr)oxides is strongly pH-dependent, the pH-dependent PFAS binding to surfaces with little or no variable charge, such as silica or clay minerals, is significantly smaller or even absent (Tang et al., 2010; Zhao et al., 2014). Possibly, this is due to significant contributions from hydrophobic interactions to the overall sorption. These may involve siloxane patches (≡Si–O–Si≡) on the mineral surfaces (Shafique et al., 2017). Hence, in soils where hydrophobic interactions with silicates are important, the binding of PFASs would be expected to be less pH-dependent compared to soils where organic matter and metal (hydr) oxides are the major sorbents.

The complex sorption behavior of PFASs results from their unique chemical structure, which consists of an ionizable hydrophilic head group and a hydrophobic organofluorine tail. Therefore, common models for predicting the sorption of non-ionizable, hydrophobic organic chemicals are not suitable for describing the sorption of PFASs to soil or other geosorbents, as electrostatic effects between sorbate and sorbent are not considered (e.g. Karickhoff et al., 1979). To address this issue, Higgins and Luthy (2007) derived a mechanistic model for PFAS binding to organic matter in sediment materials, which considers both hydrophobic and electrostatic interactions. In their approach, the K_d value was related to the PFAS-specific hydrophobicity, the organic carbon content of the sorbent, and the coulombic (electrostatic) free energy contribution, which was expressed as a Donnan potential between the organic matter fraction and the aqueous phase. The electrostatic contribution was calculated as a function of specific aqueous conditions, i.e., pH and dissolved ionic concentrations using a non-ideal competitive adsorption (NICA) Donnan model. Although theoretically sound, the model has, to the best of our knowledge, not yet been applied on soil materials. In previous work, a similar approach was used to relate the binding of PFASs to "pure" organic soil materials (O horizon and *Sphagnum* peat) to their net surface charge under varying soil solution conditions (Campos-Pereira et al., 2022, 2018). The net surface charge of the organic matter was calculated using the Stockholm Humic Model, SHM (Gustafsson, 2001). In mineral soils, the presence of cations such as Fe^{3+} and Al^{3+} will strongly affect the surface charge of the organic component; this effect can be estimated using SHM. Thus, in the current work we use SHM to explore the possibility that PFAS partitioning in a diverse set of mineral soils is determined by the net surface charge of the organic matter. To our knowledge this is the first time that PFAS partitioning of mineral soils has been predicted by a state-of-the-art model for proton and cation binding using relationships between log K_d and net surface charge as obtained for pure organic matter samples.

The specific objectives were i) to determine the pH-dependent binding of six PFASs of environmental concern that are commonly detected in soils (PFOA, PFDA, PFUnDA, PFHxS, PFOS and FOSA), ii) to ealuate how specific and multiple soil properties influence the binding, and iii) to investigate whether it is possible to model PFAS binding to mineral soils using surface charge-dependent organic carbon-normalized soil–water partitioning coefficients (K_{OC} values) determined for soil organic matter. 11 temperate soils having a wide range of key soil properties (pH, OC, clay and Fe/Al (hydr)oxides) are used in this investigation.

2. Materials and methods

2.1. Chemicals and reagents

Six PFASs were included in this study: perfluorooctanoate (PFOA), perfluorodecanoate (PFDA), perfluoroundecanoate (PFUnDA), perfluorohexane sulfonate (PFHxS), perfluorooctane sulfonate (PFOS), and perfluorooctane sulfonamide (FOSA). The selected compounds represent PFASs of environmental concern frequently found in soils (Brusseau et al., 2020), as well as in groundwaters (Johnson et al., 2022) and in bulk deposition (Cousins et al., 2022). Details on the studied PFASs (purities ≥98%, purchased from Sigma Aldrich, Saint Louis, MO) and the associated isotopically labeled internal standards (ISs) (purities >98%, Wellington Laboratories, Guelph, ON), used for quantification and quality assurance and control (QA/QC), are provided in Appendix A, Table A1. Sodium nitrate ($NaNO_3$) and Titrosol® solutions of nitric acid (HNO_3) and sodium hydroxide (NaOH) were purchased from Merck, Darmstadt. All solvents, including MeOH (LiChrosolv hypergrade®, Merck, Darmstadt), were of analytical grade.

2.2. Soil sample collection and characterization

Eleven temperate soils were chosen to represent a wide range of soil properties such as OC (0.19–3.1%), pH(H_2O) (4.6–8.3), concentrations of oxalate- and pyrophosphate-extractable Fe and Al, C/N ratio (8–40), texture (sand, silt and clay), cation exchange capacity (0.45–20 $cmol_c$ kg^{-1}) and inorganic C (0–0.3%) (Table 1, Table A.2). The soils were labeled from S1 to S11 in order of decreasing OC content, i.e., soil S1 had

the highest OC content.

2.3. Spiking and aging of soils

A sample of field-moist soil, weighing 40 g on a dry weight (dw) basis, was added to 250 mL high-density polyethylene (HDPE) containers. To each soil sample, a mixture of the studied PFASs dissolved in analytical grade methanol (MeOH) was added dropwise (in total 2 mL) to yield soil concentrations of 104 ± 27 μg kg^{-1} (dw) each of PFOA, PFHxS, PFOS, and FOSA, and 33 ± 7.5 μg kg^{-1} (dw) of PFDA and PFUnDA (as shown in Table A.3). The spiking concentrations were low enough to ensure that the binding of all PFASs occurred in the linear range in the experiment (Milinovic et al., 2015; Campos-Pereira et al., 2022). After spiking, each container with soil was left open to air to allow the MeOH to evaporate, after which the material was thoroughly/mixed and the containers were tightly capped. The spiked soils were aged for nine months in darkness at +4° C before the start of the experiment.

In addition to the laboratory-spiked soils, one field-contaminated soil (soil S3, Arboga (field-contaminated); 63 μg PFOS kg^{-1} dw, 6.4 μg PFHxS kg^{-1} dw) was included in the experiment (Table A.4). To allow for comparison of PFAS sorption between the field and the laboratory, an uncontaminated soil (S5 Arboga) was sampled in close proximity (~30 m) to the field-contaminated site (Table 1) and subsequently spiked as described above.

For the soil samples, total soil PFAS concentrations were determined by two commercial laboratories (Eurofins, ALS Scandinavia). The extracted total concentrations were, on average, 98 (±16)% of that of the methanolic spike used for quantification of the partitioning in the batch experiments (Table A3). However, for the soil with the lowest OC content (soil S11, Riddarhyttan 10–20 cm), only 67% of the spike concentration, on average, was recovered in the soil extracts. This was likely due to the low retention capacity of this soil, which was caused by its low OC content and high sand content (see Results and Discussion section). As a result, the partitioning of PFASs in this soil was quantified based on its extracted total concentrations after aging. For soils S1 and S9 (Kungsängen 0–10 cm, and Kungsängen 70–80 cm, respectively), all of the soil material was used in the sorption experiments, which is why no experimental extraction of total PFAS concentrations was performed on these soils.

2.4. pH-dependent batch experiments

2.00 g dw soil was added to 50 mL polypropylene (PP) Corning Falcon reactors (nonpyrogenic). The soils were suspended in a mixture of Milli-Q water (analytical grade, filtered through a powdered activated carbon filter) and $NaNO_3$ solution. Various amounts of acid (HNO_3) or base (NaOH, prepared on the same day) were then added to reach a number of evenly distributed solution pH values that ranged from 3.1 to 8.6 after equilibration. The concentrations added ranged from 0 to 70 mmol kg^{-1} as HNO_3, and from 0 to 50 mmol kg^{-1} as NaOH. The additions of $NaNO_3$ stock solution (0.03 M) were adjusted to maintain the nitrate (NO_3^-) concentration at 10 mM across all pH values. All batch reactors were set up in duplicate, with a total solution volume of 20 mL and a liquid-to-soil (L/S) ratio of 10 mL g^{-1} dw soil. The reactors were equilibrated end-over-end at 45 rpm and 22 °C for 7 days, a time that has been shown to be sufficient to reach sorption equilibrium (Mejia-Avendaño et al., 2020; Zhi and Liu, 2018; Johnson et al., 2007). After equilibration, the reactors were centrifuged at 2500*g*. After centrifugation, aqueous-phase aliquots for PFAS analysis were collected and stabilized with MeOH. Subsequently, pH was measured in the supernatant using a Red Rod Ag/AgCl electrode. After filtration (0.45 μm), the aqueous concentrations of inorganic constituents (Al, Fe, Ca, Mg, Mn, K) were determined using inductively coupled plasma optical emission spectroscopy (ICP-OES, PerkinElmer Avio 200). Further details on the PFAS analysis can be found in sections SI-1 and SI-2 in Appendix A.

2.5. Data analysis

The binding of PFASs to soils was determined as the difference between added PFASs and PFAS concentrations in the aqueous phase after equilibration (desorption). The soil–water partitioning coefficient K_d (mL g^{-1} dw; Table A.7) was calculated according to Eq. (1):

$$K_d = \frac{C_{s,i} - LS \cdot C_W}{C_W} \quad (1)$$

where $C_{s,i}$ denotes the initial soil concentration (ng g^{-1} dw) prior to desorption (i.e., the spike concentration, except for soil S11), *LS* is the liquid-to-soil ratio of the reactor (10 mL g^{-1} dw) and C_W [ng mL^{-1}] is the aqueous PFAS concentration measured after equilibration. The organic

Table 1
Selected properties of soils S1–S11 that were used for the experiments.

Soil	Collection site[a]	OC (%)[b]	C/N[c]	pH (H_2O)[d]	Fe_{Ox}[e] (mmol kg^{-1})	Al_{Ox}–Al_{Pyp}[f] (mmol kg^{-1})	CEC[g] ($cmol_c$ kg^{-1})	Sand (%)[h]	Silt (%)[h]	Clay (%)[h]	Textural class
S1	Kungsängen (0–10 cm)	3.1	10	5.9[i]	180	50	20	4.2	53	43	Clay
S2	Paskalampa Bs	2.2	42	5.5	130	500	1.7	54	42	4	Sandy loam
S3	Arboga (field-contaminated)	1.7	11	6.9	130	42	13	24	26	50	Clay
S4	Fors	1.6	11	8.2[i]	34	28	15	27	56	16	Silt loam
S5	Arboga	1.3	11	5.5	110	31	8.6	27	44	29	Clay
S6	Nåntuna	1.2	11	8.3[i]	37	27	14	80	15	4.4	Sandy loam
S7	Krusenberg	1.2	13	5.5	24	12	2.6	86	8	6	Loamy sand
S8	Paskalampa E	1.1	40	4.6	2.5	1.9	1.8	53	40	7	Sandy loam
S9	Kungsängen (70–80 cm)	0.91	8.0	6.6	200	51	16	0.68	48	52	Clay
S10	Högåsa (subsoil)	0.30	17	5.8	30	28	0.77	89	8	3	Loamy sand
S11	Riddarhyttan (10–20 cm)	0.19	n.a.	5.3	22	80	0.45	96	3	2	Sand

[a] All soils were from surface horizons (i.e. from the top 10 or 20 cm) with the exception of soils S2, S8, S9 and S10.
[b] OC: organic carbon content.
[c] Mass ratio.
[d] Determined according to ISO 10390:2005 at a liquid-to-soil ratio of 5 mL g^{-1} dw.
[e] Fe_{Ox}: oxalate-extractable iron (0.2 M oxalate, pH 3.0).
[f] $Al_{Ox.}$–Al_{Pyp}: The difference between oxalate-extractable aluminum (0.2 M oxalate, pH 3.0) and pyrophosphate-extractable (0.1 M) aluminum.
[g] Cation exchange capacity, determined with the hexaamminecobalt (III) chloride (CoHex) method with correction for organic matter absorbance.
[h] Determined according to ISO 11277:2020 by means of laser diffraction. [i]The soil contained inorganic carbon (Table A2). n. a.: not available. Additional details are provided in Appendix A, section SI-2.

carbon-normalized soil–water partitioning coefficient K_{OC} (mL g^{-1}) was calculated from K_d and the fraction of soil organic carbon, f_{OC} (unitless), according to Eq. (2) (see results in Table A.8):

$$K_{OC} = \frac{K_d}{f_{OC}} \quad (2)$$

According to the Shapiro-Wilk text (Shapiro and Wilk, 1965), the logarithms of K_d and K_{OC} were generally normally distributed. Therefore, descriptive statistics of the partitioning data were calculated based on the log-transformed partitioning coefficients. The average pH value of all analyzed samples was 5.7, which is close to the average pH(H_2O) of the soils (6.2).

Single (SLR) and multiple linear regression (MLR) were used to examine relationships between PFAS binding and soil properties at a fixed pH value of 5.6 ± 0.1, which reflects the average pH of all samples. The MLR models initially included the candidate predictors of OC, silt + clay content, Fe_{Ox}, and Al_{Ox-Pyp}, and non-significant predictors ($p > 0.05$) were sequentially removed, starting with the one with the highest p value. The final MLR models only include predictors with partial slopes that are significantly different from zero ($p \leq 0.05$). Further details on the MLR methods can be found in section SI-5 and in Table A.12.

2.6. Geochemical modeling

To further investigate the role of soil organic matter (SOM) for the sorption of PFASs, the Stockholm Humic Model (SHM) (Gustafsson, 2001) was used to estimate the pH-dependent surface net charge of the SOM fraction for each soil. These calculations were carried out using the chemical equilibrium software Visual MINTEQ (Gustafsson, 2022), with the assumption that only SOM was contributing to PFAS binding. The procedures for calculating the SOM net charge and the assumptions used are detailed in Appendix A, section SI-4. The calculated SOM net charge was then related to the charge-dependent PFAS sorption (K_{OC}), as found for the peat Oe material of Campos-Pereira et al. (2022). By assuming that the charge-K_{OC} relationship for the studied soils was the same as in the peat Oe sample, which consisted almost exclusively of SOM, we were able to predict charge-corrected K_{OC} values ($K_{OC,\ pred}$) for soil S1–S11. The compound-specific partitioning data and regression statistics (i.e., the relationship between SOM net charge and log K_{OC}) are provided in Table A.14 and Fig. A.1. The predicted K_d values ($K_{d,\ pred}$) for soils S1–S11 were obtained from $K_{d,\ pred} = K_{OC,\ pred} \cdot f_{OC}$, where f_{OC} is the fraction of organic carbon of the soil.

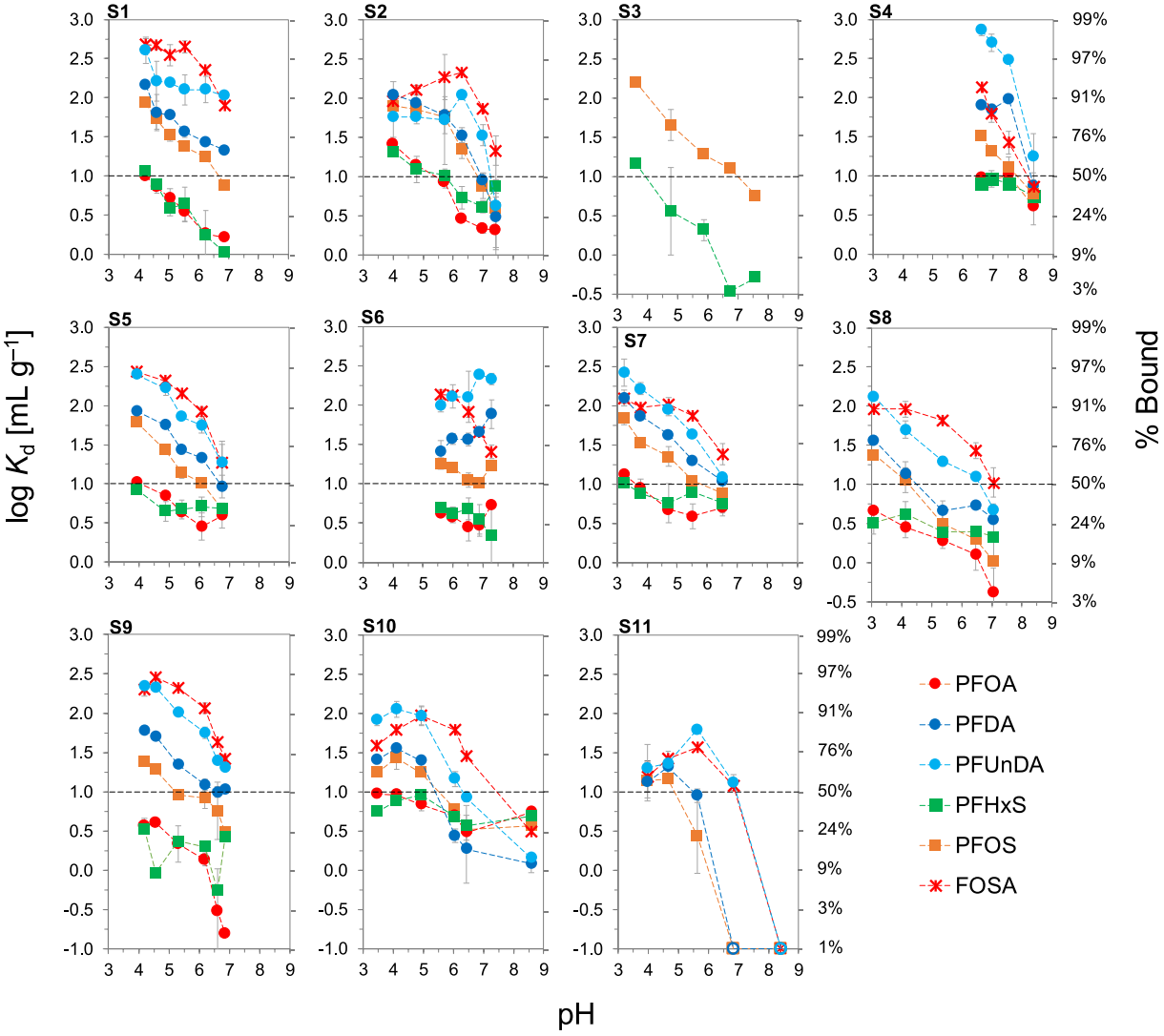

Fig. 1. Logarithmic soil–water partitioning coefficients, log K_d (mL g^{-1}), for PFASs in soils S1–S11 as a function of pH (L/S ratio: 10 mL g^{-1} dw soil). Log K_d values of −1, 0, 1, 2 and 3 correspond to a particulate-bound fraction of 1%, 9%, 50% (horizontal dashed line), 91% and 99%, respectively. The open symbols for PFDA, PFUnDA, PFOS and FOSA at high pH of soil S11 mean that the sorbed fraction was 0%. $n = 2$ replicates for all data points.

3. Results and Discussion

3.1. Soil–water partitioning of PFASs

The binding of PFASs varied by several orders of magnitude depending on the substance and the pH value (Fig. 1, Tables A.6 and A.7, Figs. A.2 – A.7). The log-normal averages (±standard error of the mean, SEM) of all K_d values across all soils and pH values were 4.0 ± 0.43 mL g^{-1} (PFOA), 21 ± 3.5 mL g^{-1} (PFDA), 58 ± 13 mL g^{-1} (PFUnDA), 4.6 ± 0.38 mL g^{-1} (PFHxS), 13 ± 2.7 mL g^{-1} (PFOS), and 62 ± 11 mL g^{-1} (FOSA) (Fig. A.8). For PFOA and PFOS, the K_d values found in this study were in the mid-range of previously reported values (0.6–9 and 5–76 mL g^{-1}, respectively) for mineral soils (with $f_{OC} \leq 7.7\%$) with similar solution compositions. The values for PFDA, PFUnDA, PFHxS, and FOSA were in the upper range of previous reports (1/4, 51, 0.9–4, and 41 mL g^{-1}, respectively) (Nguyen et al., 2020; Knight et al., 2019, 2021; Umeh et al., 2021; Milinovic et al., 2015; Mejia-Avendaño et al., 2020; Guelfo and Higgins, 2013; Enevoldsen and Juhler, 2010, Fabregat-Palau et al., 2021). The log K_d values increased with the length of the perfluorinated carbon chain for the subclasses of PFCAs and PFSAs (Fig. 1, Fig. A.8), with, on average, 0.38 and 0.23 log units per additional CF_2 moiety. The positive relationship between chain length/molecular weight and K_d (Fig. A.9) may indicate that hydrophobic interaction with, e.g., SOM, was the principal mechanism responsible for the overall sorption of each of the six PFASs in this study. However, longer-chained PFASs may also bind more strongly to Fe and Al (hydr)oxides through electrostatic interactions (Johnson et al., 2007; Campos-Pereira et al., 2020).

3.2. Effect of solution pH on partitioning

The partitioning of all analyzed substances was inversely related to solution pH in the majority of the individual soils ($p < 0.05$), with the average regressed linear slope ΔK_d for each substance–soil pair being −0.29 log units per pH unit (Fig. 1, Table A10). Acidic pH values increased the partitioning towards the solid phase for all studied PFASs, while neutral or alkaline pH values (i.e., pH 7–8.6) resulted in lower K_d values (for more details see Table A7 and Figs. A2-A8). The magnitude of the effect of pH on partitioning varied significantly depending on the substance and soil in question (Fig. 1). The largest effect of pH on PFAS partitioning was observed in the sandy OC-poor soil S11 (average slope across all substances: 0.63 log units per unit pH) followed by the alkaline calcareous silt loam soil S4 (average slope: 0.50 log units per unit pH).

The linear regression slope between log K_d and pH also depended on the PFAS, becoming steeper (i.e., more negative) with increasing perfluorocarbon chain length ($p < 0.05$, $r^2 = 0.75$) (Fig. 2, Table A10), similar to the observations of Nguyen et al. (2020). As none of the investigated PFASs except FOSA dissociates over the studied pH range (~3–9), the pH-dependent nature of PFAS sorption was attributed to the variable charge of the solid phase (i.e., the lower the net negative charge, the stronger the sorption). The steeper log K_d-pH slope for longer-chained PFASs is consistent with the stronger contribution of electrostatic interactions between the electronegative fluorines of the tail part of the molecules and the soil particles (Erkoç and Erkoç, 2001; Johnson et al., 2007; Xiao et al., 2011; Park et al., 2020). The proposed nature of the pH dependence is also consistent with previous work on the pH-dependent sorption of PFASs to organic soil materials and to the iron (hydr)oxide ferrihydrite (Campos-Pereira et al. 2020, 2022Campos-Pereira et al. 2022). However, the log K_d-pH slope is steeper for these "pure" materials compared to those obtained for the mineral soils in the present study, which might indicate a contribution from an unknown solid phase to PFAS binding, probably through hydrophobic interactions.

In contrast to the other PFASs under study, the sorption of FOSA was influenced by its dissociation near its pK_a value (acid dissociation constant), which is in agreement with the study conducted by Nguyen et al. (2020). The pK_a of FOSA has been estimated to be 6.24 (Rayne and Forest, 2009) or 6.52 (Steinle-Darling and Reinhard, 2008). At pH values below the pK_a, FOSA was strongly bound (≥79% across all soils; Fig. A.7; Table A.9) in its undissociated form. However, at pH values above the pK_a, FOSA was predominantly present in its dissociated form ($C_8F_{17}SO_2NH^-$) and exhibited similar behavior to that of its anionic C_8 analog PFOS (Fig. 1, Fig. A.10).

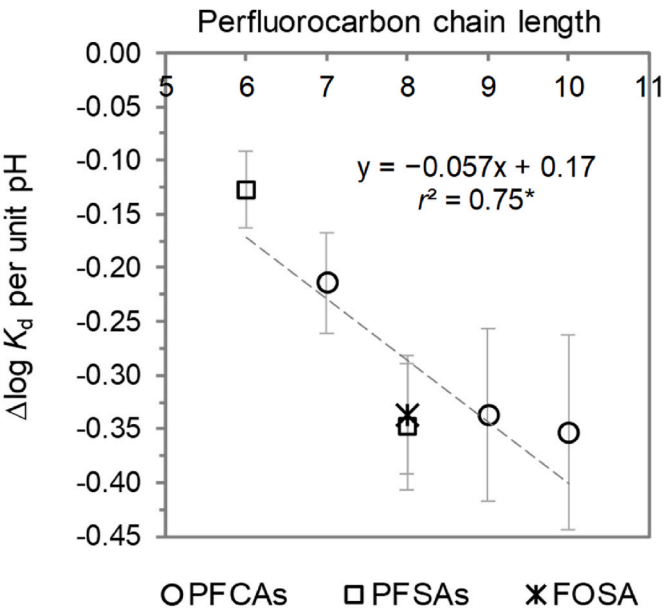

Fig. 2. Slope of the log K_d–pH relationship as influenced by the length of the perfluorinated carbon chain. For each PFAS, the average of the regression slope (Δlog K_d per pH unit) for all 10 laboratory-spiked soils is shown. Error bars represent the standard error of the mean. *$p \leq 0.05$.

3.3. Effects of soil properties on partitioning

In general, the PFASs under study tended to be sorbed more strongly to soils that had higher OC content, higher silt and clay contents, higher extractable Fe_{Ox} and $Al_{Ox–Pyp}$, and were surface rather than subsurface horizons, which is in line with previous research and demonstrates the complex behavior of PFAS sorption (Knight et al., 2019, 2021; Nguyen et al., 2020; Umeh et al., 2021). However, only a few of the aforementioned K_d–soil property relationships were statistically significant ($p \leq 0.05$) for individual PFASs in the current study (Table A12).

Single linear regression (SLR) at pH 5.6 ± 0.1 showed that several soil properties had significant ($p \leq 0.05$) positive correlations with the K_d value for some of the PFASs, including OC (FOSA), oxalate-extractable Fe, i.e., Fe_{Ox} (FOSA), $Al_{Ox–Pyp}$ (PFOS, PFDA), the sum of Fe_{Ox} and Al_{Ox-Pyp} (PFOS, PFDA), CEC (FOSA), the combined content of silt and clay (FOSA), and total N content (FOSA) (Table A12). Although these relationships were significant, their predictive strength was weak to moderate (average $r^2 = 0.58$). Normalizing PFAS partitioning against OC (K_{OC} or log K_{OC}) did not successfully explain the differences in PFAS sorption between soils (Table A.8; Fig. A.11 and A.12). Additionally, the experimentally determined K_{OC} value (assuming that organic matter was the only sorbent) was significantly greater for the mineral soils (often >1 log unit greater for PFHxS, PFOS, PFOA and FOSA) than for the organic soil materials (Fig. 3 and Fig. A.12), indicating that extrapolating K_{OC} values from organic soil materials would likely underestimate the binding of the PFASs to mineral soils.

For PFOS and FOSA, multiple linear regression (MLR) models explained a larger portion of the variance in the K_d values at pH 5.6 ± 0.1 (Fig. 4, Fig A.14). Again, this suggests that multiple soil properties play a role in the sorption of PFOS and FOSA, as previously shown by Nguyen et al. (2020), Umeh et al. (2021) and Knight et al. (2021) for

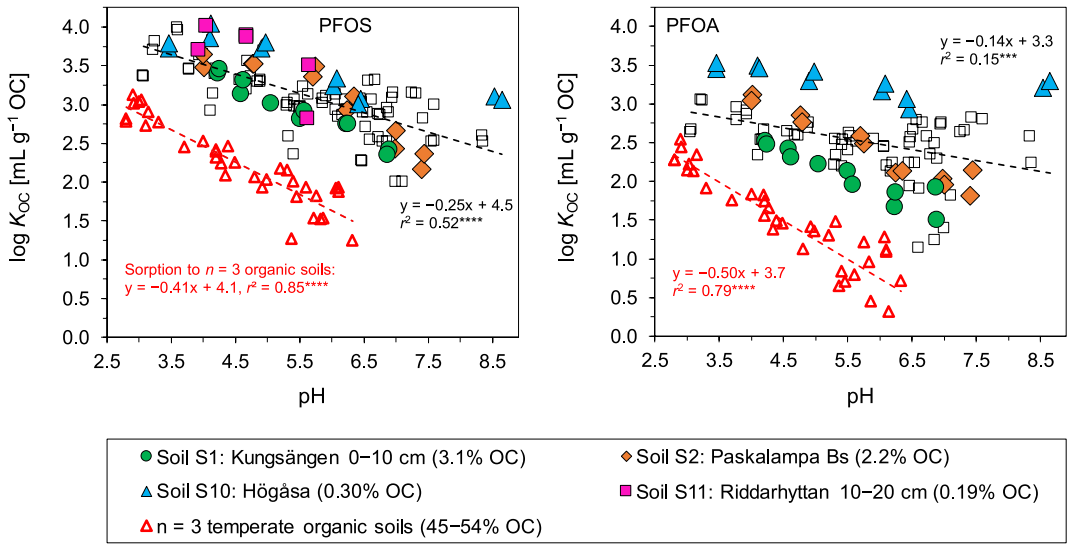

Fig. 3. Organic carbon-normalized partitioning coefficients log K_{OC} (mL g^{-1} OC) for PFOS and PFOA for all soils, where open squares represent values for soils S3-S9, and for 3 organic soils (open red triangles, data from Campos-Pereira et al., 2022). Additional plots for PFHxS, PFUnDA and FOSA are provided in Fig. A.11. ****$p \leq$ 0.0001, ***$p \leq$ 0.001.

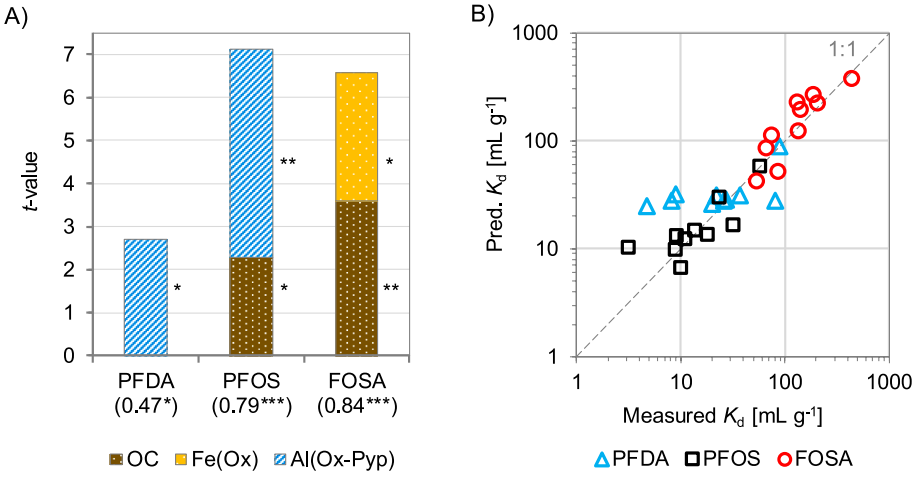

Fig. 4. A) t-values of soil properties of significant multiple linear regression (MLR) models describing the K_d values at pH 5.6 ± 0.1 in 10 laboratory-spiked soils. Adjusted r^2 values for MLR models are given in parenthesis. *p ≤ 0.05, **p ≤ 0.01, ***p ≤ 0.001. All the partial slopes of the MLR models were significantly different from zero (p ≤ 0.05). No significant relationships were found for PFOA, PFUnDA and PFHxS, why these substances are not included in figure. B) Fits of statistical models (log–log scale, pH 5.6 ± 0.1), shown as predicted K_d plotted against measured K_d for PFDA, PFOS and FOSA.

anionic PFASs including PFOS. For both PFOS and FOSA, OC was positively correlated with the K_d value ($p \leq 0.05$), as previously found by Nguyen et al. (2020) and Umeh et al. (2021). Both the SLR and MLR analysis suggested that $Al_{Ox–Pyp}$ played a role in the binding of PFOS, while Fe_{Ox} played a role in the binding of FOSA. Together with OC, these parameters explained 79% and 84% of the variance in the measured K_d values of PFOS and FOSA, respectively (Fig. 4). In contrast, Nguyen et al. (2020) did not identify any significant predictor associated with the mineral fraction for the sorption of PFOS, FOSA, and PFDA, with the exception of the soil micropore volume. Instead, these authors reported OC as the only significant predictor for the sorption of these three substances. A strong role of OC concerning the sorption of PFASs was also reported by other studies (e.g., Knight et al., 2019; Nguyen et al., 2020; Oliver et al., 2020). In our study, OC was not a significant predictor of sorption for any of the three investigated PFCAs (i.e., PFOA, PFDA, PFUnDA), nor for PFHxS. Li et al. (2019) proposed that the protein component of soil organic matter might be a better predictor of PFAS sorption than OC. However, our results indicate that total N was not a better predictor than OC for PFAS sorption (Fig. A12), which does not support this hypothesis.

PFOS was sorbed approximately twice as strongly in the field-contaminated soil S3 (Arboga field-contaminated) compared to in the laboratory-spiked soil S5 (Arboga; Fig. 1, A5 and A6). Considering the somewhat higher organic carbon and clay contents in the field-contaminated soil (Table 1), the results suggest that the effect of aging in the field was not a major factor affecting the soil–water partitioning of PFOS.

3.4. Partitioning as predicted from modeled SOM net charge

The modeling approach of applying surface charge-dependent K_{OC} values for a peat (Oe) material to account for pH-dependent PFAS binding (i.e., Δlog K_d per pH unit) in mineral soils resulted in satisfactory agreement in only a few cases (Fig. 5, Fig. A.14). FOSA was followed by PFOA as the PFASs for which the model exhibited the best overall performance. However, in the large majority of soils, the K_d values were considerably underestimated. The best model fit was observed for soil S2 (Paskalampa Bs); predicted K_d values were, on averae, 2.5 (±2.5) times lower than those measured for PFOA, PFUnDA, PFHxS, PFOS, and FOSA (PFDA sorption was not predicted, as calibration data for the peat Oe material was not available). The largest deviations from the modeled partitioning were observed for the Arboga clay soils S3 (impacted by aqueous film-forming foam, AFFF) and S5. For these two soils, the model underestimated the partitioning by a factor of 40 (±2.5).

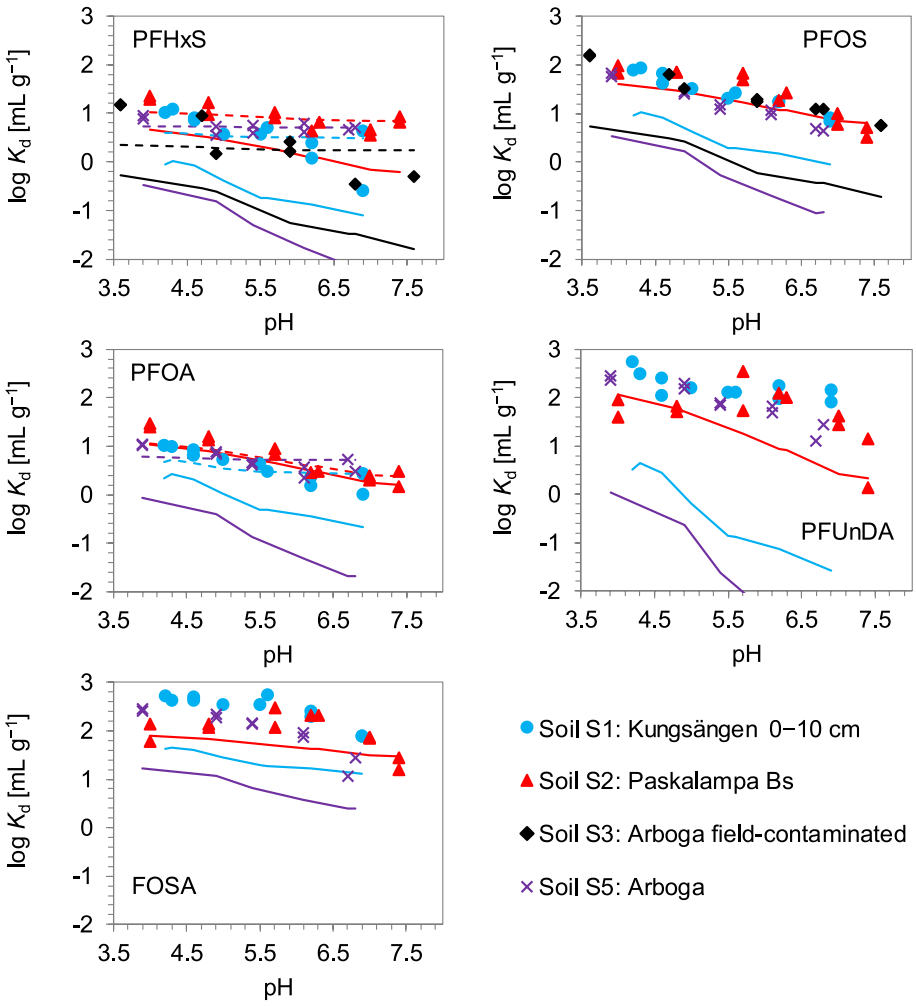

Fig. 5. Measured soil–water partitioning (points) for selected soils and partitioning predicted from SOM net charge (solid lines). For PFOA and PFHxS, partitioning was also predicted from the sum of SOM net charge-normalized sorption and a pH-independent sorption contribution (dashed lines).

The fact that the model underestimated the measured partitioning for all soils to varying degrees indicates that there is an important retention mechanism, or possibly an unknown interaction effect, that is not captured by the model. One such mechanism could be the involvement of hydrophobic sorption to silicate minerals, as reported for C_7–C_{11} PFCAs and PFOS in isolated systems of silica particles (Shafique et al., 2017; Tang et al., 2010). To explore this possibility, for PFOA and PFHxS, we included a hypothetical pH-independent sorption contribution of a silicate phase with $K_d = 4.0 \pm 2.0$ L kg soil^{-1}, where the exact value was allowed to depend on the soil and the PFAS compound. This greatly improved the overall model fit for these two substances (dashed lines in Fig. 5, Fig. A.15). However, without direct evidence, the assignment of a silicate sorption contribution remains speculative. Alternatively, the possible presence of a high-affinity sorbent component, such as black carbon or other pyrogenic carbonaceous materials (Zhi and Liu, 2018), may produce the observed difference between predicted and measured partitioning. However, this would require that such high-affinity phases were present in all mineral soils (possibly excluding soil S2), but not in the peat (Oe) material used for calibrating the model, which is less likely.

4. Conclusions

The overall sorption of PFASs was positively correlated with the perfluorocarbon chain length of the molecule, indicating that hydrophobic sorption to the solid phase was the main mechanism responsible for PFAS binding. Furthermore, the binding of all PFASs was inversely proportional to the solution pH, indicating that electrostatic interactions with the solid phase play a significant role in their binding. The pH dependence of sorption was greater for longer-chained PFASs compared to shorter-chained substances, suggesting that the perfluorinated tail, as well as the head group, affects PFAS sorption through electrostatic interactions with the sorbent.

The sorption of PFASs to mineral soils was considerably underestimated when extrapolated from organic soil materials using OC content or SOM net charge. Thus, a model that predicts PFAS sorption solely from OC characteristics is unlikely to be successful for mineral soils. Minerogenic components also appear to contribute significantly to PFAS sorption in mineral soils, but the magnitude and mechanisms require further investigation. More research is needed to understand the PFAS sorption mechanisms to enable the development of geochemical models capable of simulating and predicting the binding of PFASs in mineral soils.

Credit author statement

Hugo Campos-Pereira: Methodology, Investigation, Writing – original draft, Visualization, Formal analysis, Writing – review and editing; **Dan B. Kleja**: Conceptualization, Writing – review and editing, Supervision. **Lutz Ahrens:** Methodology, Resources, Writing – review and editing, Supervision; **Anja Enell:** Investigation, Writing – review and editing; **Johannes Kikuchi:** Investigation, Writing – review and

editing; **Michael Pettersson:** Resources, Writing – review and editing, Supervision; **Jon Petter Gustafsson:** Conceptualization, Software, Writing – review and editing, Supervision, Project administration, Funding acquisition.

Declaration of competing interest

The authors declare that they have no known competing financial interests or personal relationships that could have appeared to influence the work reported in this paper.

Data availability

Data will be made available on request.

Acknowledgments

The authors wish to thank the Swedish Research Council VR (Vetenskapsrådet, grant number 2015-03938) and the Swedish Geotechnical Institute for funding this research. The authors are grateful to Gbotemi Adediran who provided soils S1 and S9 to this study, to Mattias Sörengård for providing soil S10, to Marius Tuyishime for providing soil S11, and to Carin Sjöstedt for valuable comments on the manuscript. Elin Ljunggren is acknowledged for analysis of soil carbon and total nitrogen, Jan Fiedler for analysis of dissolved metals, and Elin Eriksson for assistance with UPLC-MS/MS instrumentation.

Appendix A. Supplementary data

Supplementary data to this article can be found online at https://doi.org/10.1016/j.chemosphere.2023.138133.

References

Brusseau, M.L., Anderson, R.H., Guo, B., 2020. PFAS concentrations in soils: background levels versus contaminated sites. Sci. Total Environ. 740, 140017 https://doi.org/10.1016/j.scitotenv.2020.140017.

Campos Pereira, H., Ullberg, M., Kleja, D.B., Gustafsson, J.P., Ahrens, L., 2018. Sorption of perfluoroalkyl substances (PFASs) to an organic soil horizon – effect of cation composition and pH. Chemosphere 207, 183–191. https://doi.org/10.1016/j.chemosphere.2018.05.012.

Campos-Pereira, H., Kleja, D.B., Sjöstedt, C., Ahrens, L., Klysubun, W., Gustafsson, J.P., 2020. The adsorption of per- and polyfluoroalkyl substances (PFASs) onto ferrihydrite is governed by surface charge. Environ. Sci. Technol. 54 (24), 15722–15730. https://doi.org/10.1021/acs.est.0c01646.

Campos-Pereira, H., Makselon, J., Kleja, D.B., Prater, I., Kögel-Knabner, I., Ahrens, L., Gustafsson, J.P., 2022. Binding of per- and polyfluoroalkyl substances (PFASs) by organic soil materials with different structural composition – charge- and concentration-dependent sorption behavior. Chemosphere 297, 134167. https://doi.org/10.1016/j.chemosphere.2022.134167.

Cousins, I.T., Johansson, J.H., Salter, M.E., Sha, B., Scheringer, M., 2022. Outside the safe operating space of a new planetary boundary for per- and polyfluoroalkyl substances (PFAS). Environ. Sci. Technol. 56 (16), 11172–11179. https://doi.org/10.1021/acs.est.2c02765.

Enevoldsen, R., Juhler, R.K., 2010. Perfluorinated compounds (PFCs) in groundwater and aqueous soil extracts: using inline SPE-LC-MS/MS for screening and sorption characterisation of perfluorooctane sulphonate and related compounds. Anal. Bioanal. Chem. 398 (3), 1161–1172. https://doi.org/10.1007/s00216-010-4066-0.

Erkoç, Ş., Erkoç, F., 2001. Structural and electronic properties of PFOS and LiPFOS. J. Mol. Struct. Theochem 549 (3), 289–293. https://doi.org/10.1016/S0166-1280(01)00553-X.

Fabregat-Palau, J., Vidal, M., Rigol, A., 2021. Modelling the sorption behaviour of perfluoroalkyl carboxylates and perfluoroalkane sulfonates in soils. Sci. Total Environ. 801, 149343 https://doi.org/10.1016/j.scitotenv.2021.149343.

Fabregat-Palau, J., Vidal, M., Rigol, A., 2022. Examining sorption of perfluoroalkyl substances (PFAS) in biochars and other carbon-rich materials. Chemosphere 302, 134733. https://doi.org/10.1016/j.chemosphere.2022.134733.

Guelfo, J.L., Higgins, C.P., 2013. Subsurface transport potential of perfluoroalkyl acids at aqueous film-forming foam (AFFF)-impacted sites. Environ. Sci. Technol. 47 (9), 4164–4171. https://doi.org/10.1021/es3048043.

Guelfo, J.L., Korzeniowski, S., Mills, M.A., Anderson, J., Anderson, R.H., Arblaster, J.A., Conder, J.M., Cousins, I.T., Dasu, K., Henry, B.J., Lee, L.S., Liu, J., McKenzie, E.R., Willey, J., 2021. Environmental sources, chemistry, fate and transport of per- and polyfluoroalkyl substances: state of the science, key knowledge gaps, and recommendations presented at the August 2019 SETAC Focus Topic Meeting. Environ. Toxicol. Chem. 40 (12), 3234–3260. https://doi.org/10.1002/etc.5182.

Gustafsson, J.P., 2001. Modeling the acid–base properties and metal complexation of humic substances with the Stockholm Humic Model. J. Colloid Interface Sci. 244 (1), 102–112. https://doi.org/10.1006/jcis.2001.7871.

Gustafsson, J.P., 2022. Visual MINTEQ – a Free Equilibrium Speciation Model.

Higgins, C.P., Luthy, R.G., 2006. Sorption of perfluorinated surfactants on sediments. Environ. Sci. Technol. 40 (23), 7251–7256. https://doi.org/10.1021/es061000n.

Higgins, C.P., Luthy, R.G., 2007. Modeling sorption of anionic surfactants onto sediment materials: an a priori approach for perfluoroalkyl surfactants and linear alkylbenzene sulfonates. Environ. Sci. Technol. 41 (9), 3254–3261. https://doi.org/10.1021/es062449j.

Jeon, J., Kannan, K., Lim, B.J., An, K.G., Kim, S.D., 2011. Effects of salinity and organic matter on the partitioning of perfluorooalkyl acid (PFAs) to clay particles. J. Environ. Monit. 13, 1803–1810. https://doi.org/10.1039/C0EM00791A.

Johnson, G.R., Brusseau, M.L., Carroll, K.C., Tick, G.R., Duncan, C.M., 2022. Global distributions, source-type dependencies, and concentration ranges of per- and polyfluoroalkyl substances in groundwater. Sci. Total Environ. 841, 156602 https://doi.org/10.1016/j.scitotenv.2022.156602.

Johnson, R.L., Anschutz, A.J., Smolen, J.M., Simcik, M.F., Penn, R.L., 2007. The adsorption of perfluorooctane sulfonate onto sand, clay, and iron oxide surfaces. J. Chem. Eng. Data 52 (4), 1165–1170. https://doi.org/10.1021/je060285g.

Karickhoff, S.W., Brown, D.S., Scott, T.A., 1979. Sorption of hydrophobic pollutants on natural sediments. Wat. Res. 13 (3), 241–248. https://doi.org/10.1016/0043-1354(79)90201-X.

Knight, E.R., Janik, L.J., Navarro, D.A., Kookana, R.S., McLaughlin, M.J., 2019. Predicting partitioning of radiolabelled 14C-PFOA in a range of soils using diffuse reflectance infrared spectroscopy. Sci. Total Environ. 686, 505–513. https://doi.org/10.1016/j.scitotenv.2019.05.339.

Knight, E.R., Bräunig, J., Janik, L.J., Navarro, D.A., Kookana, R.S., Mueller, J.F., McLaughlin, M.J., 2021. An investigation into the long-term binding and uptake of PFOS, PFOA and PFHxS in soil – plant systems. J. Hazard Mater. B404, 124065 https://doi.org/10.1016/j.jhazmat.2020.124065.

Li, F., Fang, X., Zhou, Z., Liao, X., Zou, J., Yuan, B., Sun, W., 2019. Adsorption of perfluorinated acids onto soils: kinetics, isotherms, and influences of soil properties. Sci. Total Environ. 649, 504–514. https://doi.org/10.1016/j.scitotenv.2018.08.209.

Li, Y., Oliver, D.P., Kookana, R.S., 2018. A critical analysis of published data to discern the role of soil and sediment properties in determining sorption of per and polyfluoroalkyl substances (PFASs). Sci. Total Environ. 628–629, 110–120. https://doi.org/10.1016/j.scitotenv.2018.01.167.

Luft, C.M., Schutt, T.C., Shukla, M.K., 2022. Properties and mechanisms for PFAS adsorption to aqueous clay and humic soil components. Environ. Sci. Technol. 56 (14), 10053–10061. https://doi.org/10.1021/acs.est.2c00499.

Mejia-Avendaño, S., Zhi, Y., Yan, B., Liu, J., 2020. Sorption of polyfluoroalkyl surfactants on surface soils: effect of molecular structures, soil properties, and solution chemistry. Environ. Sci. Technol. 54 (3), 1513–1521. https://doi.org/10.1021/acs.est.9b04989.

Milinovic, J., Lacorte, S., Vidal, M., Rigol, A., 2015. Sorption behaviour of perfluoroalkyl substances in soils. Sci. Total Environ. 511, 63–71. https://doi.org/10.1016/j.scitotenv.2014.12.017.

Nguyen, T.M.H., Bräunig, J., Thompson, K., Thompson, J., Kabiri, S., Navarro, D.A., Kookana, R.S., Grimison, C., Barnes, C.M., Higgins, C.P., McLaughlin, M.J., Mueller, J.F., 2020. Influences of chemical properties, soil properties, and solution pH on soil–water partitioning coefficients of per- and polyfluoroalkyl substances (PFASs). Environ. Sci. Technol. 54 (24), 15883–15892. https://doi.org/10.1021/acs.est.0c05705.

Oliver, D.P., Li, Y., Orr, R., Nelson, P., Barnes, M., McLaughlin, M.J., Kookana, R.S., 2019. The role of surface charge and pH changes in tropical soils on sorption behaviour of per- and polyfluoroalkyl substances (PFASs). Sci. Total Environ. 673, 197–206. https://doi.org/10.1016/j.scitotenv.2019.04.055.

Oliver, D.P., Navarro, D.A., Baldock, J., Simpson, S.L., Kookana, R.S., 2020. Sorption behaviour of per- and polyfluoroalkyl substances (PFASs) as affected by the properties of coastal estuarine sediments. Sci. Total Environ. 720, 137263 https://doi.org/10.1016/j.scitotenv.2020.137263.

Park, M., Daniels, K.D., Wu, S., Ziska, A.D., Snyder, S.A., 2020. Magnetic ion-exchange (MIEX) resin for perfluorinated alkylsubstance (PFAS) removal in groundwater: roles of atomic charges for adsorption. Wat. Res. 181, 115897 https://doi.org/10.1016/j.watres.2020.115897.

Rayne, S., Forest, K., 2009. A new class of perfluorinated acid contaminants: primary and secondary substituted perfluoroalkyl sulfonamides are acidic at environmentally and toxicologically relevant pH values. J. Environ. Sci. Health A44 (13), 1388–1399. https://doi.org/10.1080/10934520903217278.

Shafique, U., Drn, V., Paschke, A., Schüürmann, G., 2017. Adsorption of perfluorocarboxylic acids at the silica surface. Chem. Commun. (J. Chem. Soc. Sect. D) 53, 589–592. https://doi.org/10.1039/C6CC07525H.

Shapiro, S.S., Wilk, M.B., 1965. An snalysis of variance test for normality (complete samples). Biometrika 52 (3/4), 591–611. https://doi.org/10.2307/2333709.

Steinle-Darling, E., Reinhard, M., 2008. Nanofiltration for trace organic contaminant removal: structure, solution, and membrane fouling effects on the rejection of perfluorochemicals. Environ. Sci. Technol. 42 (14), 5292–5297. https://doi.org/10.1021/es703207s.

Tang, C.Y., Fu, Q.S., Gao, D., Criddle, C.S., Leckie, J.O., 2010. Effect of solution chemistry on the adsorption of perfluorooctane sulfonate onto mineral surfaces. Wat. Res. 44, 2654–2662. https://doi.org/10.1016/j.watres.2010.01.038.

Umeh, A.C., Naidu, R., Shilpi, S., Boateng, E.B., Rahman, A., Cousins, I.T., Chadalavada, S., Lamb, D., Bowman, M., 2021. Sorption of PFOS in 114 well-characterized tropical and temperate soils: application of multivariate and artificial

neural network analyses. Environ. Sci. Technol. 55 (3), 1779–1789. https://doi.org/10.1021/acs.est.0c07202.

Wang, F., Shih, K., 2011. Adsorption of perfluorooctanesulfonate (PFOS) and perfluorooctanoate (PFOA) on alumina: influence of solution pH and cations. Wat. Res. 45, 2925–2930. https://doi.org/10.1016/j.watres.2011.03.007.

Xiao, F., Zhang, X., Penn, L., Gulliver, J.S., Simcik, M.F., 2011. Effects of monovalent cations on the competitive adsorption of perfluoroalkyl acids by kaolinite: experimental studies and modeling. Environ. Sci. Technol. 45 (23), 10028–10035. https://doi.org/10.1021/es202524y.

Zhao, L., Bian, J., Zhang, Y., Zhu, L., Liu, Z., 2014. Comparison of the sorption behaviors and mechanisms of perfluorosulfonates and perfluorocarboxylic acids on three kinds of clay minerals. Chemosphere 114, 51–58. https://doi.org/10.1016/j.chemosphere.2014.03.098.

Zhi, Y., Liu, J., 2018. Sorption and desorption of anionic, cationic and zwitterionic polyfluoroalkyl substances by soil organic matter and pyrogenic carbonaceous materials. Chem. Eng. J. 346, 682–691. https://doi.org/10.1016/j.cej.2018.04.042.